

## MODELING OF A SOLAR PHOTOVOLTAIC WATER PUMPING SYSTEM UNDER THE INFLUENCE OF PANEL COOLING

by

**Gopal CHINATHAMBI<sup>a</sup>, Mohanraj MURUGESAN<sup>b,\*</sup>,  
Chandramohan PALANISAMY<sup>c,d</sup>, Sakthivel MUNIRAJAN<sup>a</sup>,  
and Shepherd BHERO<sup>c</sup>**

<sup>a</sup> Department of Mechanical Engineering, Info Institute of Engineering, Coimbatore, India

<sup>b</sup> Department of Mechanical Engineering, Hindusthan College of Engineering  
and Technology, Coimbatore, Tamil Nadu, India

<sup>c</sup> Department of Metallurgy, University of Johannesburg, Johannesburg, South Africa

<sup>d</sup> Department of Mechanical Engineering, Sri Ramakrishna Engineering College,  
Coimbatore, Tamil Nadu, India

Original scientific paper

<https://doi.org/10.2298/TSCI17S2399C>

*In this paper, the performance of a solar photovoltaic water pumping system was improved by maintaining the cell temperature in the range between 30 °C and 40 °C. Experiments have been conducted on a laboratory experimental set-up installed with 6.4 m<sup>2</sup> solar panel (by providing air cooling either on the top surface or over the beneath surface of the panel) to operate a centrifugal pump with a rated capacity of 0.5 HP. The performance characteristics of the photovoltaic panel (such as, cell temperature, photovoltaic panel output, and photovoltaic efficiency), pump performance characteristics (such as pump efficiency and discharge), and system performance characteristics are observed with reference to solar irradiation, ambient temperature and wind velocity. A thermal model has been developed to predict the variations of photovoltaic cell temperature based on the measured glass and tedlar temperatures. The influences of cell temperature and solar irradiation on the performance of the system are described. The results concluded that cooling of photovoltaic panel on beneath surface has maintained the cell temperature in the range between 30 °C and 40 °C and improved the overall efficiency by about 1.8% when compared to the system without panel cooling.*

Key words: *photovoltaic assisted water pumping systems, air cooling, modeling*

### Introduction

In India, electrical and diesel-powered water pumping systems are commonly used in agricultural sectors due to its flexibility in usage [1]. However, connecting the grid electricity with water pumping systems in the remote locations is more expensive and the usage of diesel powered water pumping systems has adverse harmful environmental impacts. Hence, the idea of integrating the solar photovoltaic panels with water pumping systems has been proposed by many researchers around the world to meet the energy demand in agricultural sectors and to reduce the adverse environmental impacts. But, the major drawback of solar

\* Corresponding author, e-mail: mohanrajbavan@gmail.com

photovoltaic water pumping systems (SPVWPS) is the performance degradation under the influence of panel heating [2]. Hence, it is essential to cool the photovoltaic panel to achieve maximum performance. In earlier investigations, the performance of a SPVWPS was improved using reflectors and panel cooling. In a related work, aluminum and stainless steel reflectors were used for performance enhancement [3]. It was reported that the average photovoltaic power output was increased by about 14% and 8.4% using aluminum and stainless steel reflectors, respectively. Similarly, Abdolzadeh and Ameri [4] improved the overall performance of a SPVWPS by sprayed water over the panel surfaces. Their results reported that, photovoltaic efficiency, subsystem efficiency and total efficiency were improved by 3.26, 1.40, and 1.35%, respectively, at a head of 16 m. Further, the performance was also improved by providing water cooling arrangement over the beneath surface of the panel [5]. The photovoltaic cell efficiency, subsystem efficiency, and total efficiency were improved by about 2, 4, and 1%, respectively. Kordzadeh [6] has significantly improved the performance of a SPVWPS by providing a film layer of water over the cell surface. Similarly, many researchers have investigated the performance of photovoltaic panels under the influence of panel cooling using air and water. Teo *et al.* [7] proposed a forced convective air cooling at the beneath surface of the photovoltaic panel and improved the electrical efficiency up to 14%. In another work, Nizetic *et al.* [8] improved the electrical efficiency of the photovoltaic panel to 14.3% under the influence of water cooling by maintaining the panel temperature around 24 °C. However, the use of water for panel cooling is not an economical option in water scarcity locations. Moreover, the cited literature confirmed that, there is no specific research has been reported on performance of SPVWPS under the influence of air cooling. Hence, an attempt has been made in this research to cool the photovoltaic panel using air. A mathematical model was developed for predicting the performance of the photovoltaic panel, pump sub system, and overall system based on measured glass and tedlar surface temperatures.

## Experiments

Experiments were carried under the meteorological conditions of Coimbatore city (latitude of 10.98 °N and longitude of 76.96 °E) in India during the year 2015.

## Experimental set-up

The schematic diagram of a SPVWPS experimental set-up is illustrated in fig. 1(a). The cooling arrangement provided at the beneath surface is depicted in fig. 1(b). The photographic view is shown in fig. 2. The specifications of a centrifugal pump and photo-voltaic panels are given in tabs 1 and 2, respectively. The SPVWPS was installed in a sump with 5,000 L water capacity. The set-up consists of a 0.5 HP centrifugal pump assisted by a variable frequency drive operated by four photovoltaic panels (with dimensions 1.6 × 1 m) of total area 6.4 m<sup>2</sup>. The maximum photovoltaic output is 1.1 kW. The pump has 3 m of suction pipe and control valve at pump discharge for varying the delivery head. Air cooling arrangement has been provided above the panel with the help of 40 W centrifugal fan. Similarly, the cooling arrangement was also provided to cool the beneath surface of the panel using 40 W axial flow fan as shown in fig. 1(b). The cells are built into a sandwich construction placed behind a glass cover sheet to provide protection from mechanical damage. The cells are encapsulated between films of polymer to protect the cells from ambient moisture. Cells are connected in series by flat strips of copper soldered onto the front face of one cell and the rear face of the next. An aluminum extruded frame was used to support the photovoltaic panel. The panel is placed at an inclination of 11° according to the latitude of the location.

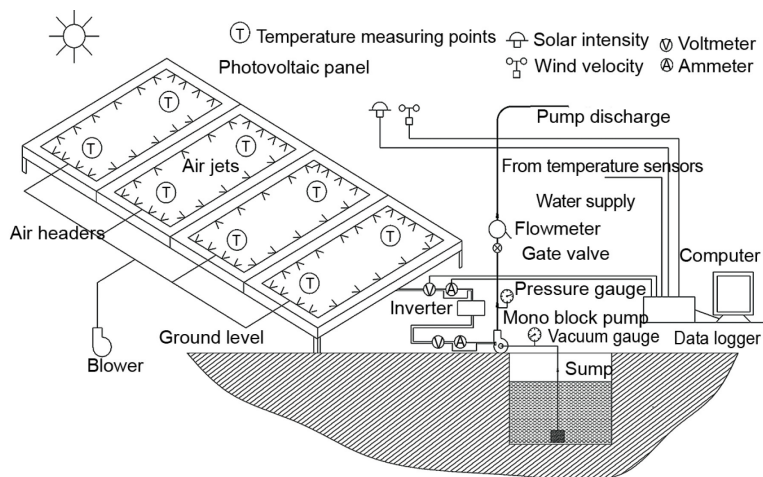


**Figure 1(a). Schematic diagram of experimental set-up (with cooling arrangement above the panel surface)**

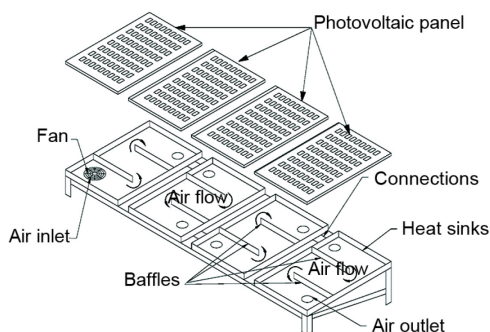


**Figure 1(b). Cooling at beneath surface of the panel**



**Figure 2. Photographic view of cooling arrangement**

### Instrumentation

Sixteen calibrated K-type thermocouples were fixed at typical locations above and below the photovoltaic panel surface to measure the glass and tedlar temperatures. Ambient wind velocity and solar irradiation were measured using a cup type anemometer and pyranometer, respectively. The instantaneous current, voltage and power outputs from the panel were measured using ammeter, voltmeter, and wattmeter, respectively. The pump discharge was measured using orifice-meter connected at the pump outlet. The power consumed by the electrical motor was measured using a separate wattmeter. All the thermocouples attached at typical locations in the photovoltaic panel surface, cup type anemometer and pyranometer are interfaced with a computer through data logger. The motor speed was measured manually using digital tachometer.

### Experimental procedure

Before conducting experiments with SPVWPS, the pump was tested using a variable frequency drive at different heads ranging from 5 to 25 m with different speeds. Polynomial equations have been developed for predicting the performance of a centrifugal pump based on

**Table 1. Specifications of water pump**

Type of motor	Single phase AC motor
Voltage, current	230 V, 2.5 A
Frequency/speed	50 Hz/2800 rpm
Power	0.5 HP and 0.375 kW
Pump	Centrifugal pump

**Table 2. Specifications of photovoltaic panel**

Voltage at $P_{max}$	35.04 V
Current at $P_{max}$	7.85 A
Open circuit voltage $V_{oc}$	43.99 V
Short circuit current $I_{sc}$	8.39 A
Temperature coefficient	-0.41% °C
Cell type	Multi crystalline
Cell size	156 mm × 156 mm
Area of the panel	6.4 m <sup>2</sup>

the preliminary lab experiments. The experimental observations were made on a SPWPS at every ten minutes interval during 9.00 a. m. to 6.00 p. m. on clear sunny days with minimum fluctuations of solar irradiation during the summer months of 2015. Frequent data observations were made in the computer to study the transient behavior of the system and also to eliminate the erroneous data. Experiments have been conducted at constant pumping head of 15 m.

#### Uncertainty analysis

The uncertainties in experimental results are calculated based on the accuracy of measuring instruments (specified in tab. 3). It is given by following equation [9]:

$$w_r = \sqrt{\left(\frac{\partial R}{\partial x_1} w_1\right)^2 + \left(\frac{\partial R}{\partial x_2} w_2\right)^2 + \dots + \left(\frac{\partial R}{\partial x_n} w_n\right)^2} \quad (1)$$

**Table 3. Specifications of the instruments**

Instrumentation	Specification (range)	Accuracy
Orifice-meter	0-100 Lpm	±2%
Temperature sensor	PT 100 (0-200 °C)	±0.2 °C
Wattmeter	Digital type	±2 W
Energy meter	Digital	±0.5%
Pyranometer	Class-A (0-1200 W/m <sup>2</sup> )	±5 W/m <sup>2</sup>
Temperature indicator	16 channel indicator	0-200 °C
Tachometer	0-3000 rpm	±5 rpm
Anemometer	0-20 m/s	±0.1 m/s
Ammeter	0-10 A	±0.1 A
Voltmeter	0-240 V	±5 V

studies [10, 11]. Hence, the modeling procedure of inverter and electrical motor are not described in this paper. A mathematical model for predicting the cell temperature under the influence of air cooling is described in this section. The model predicts the cell temperature based on the measured glass and tedlar temperatures. The photovoltaic power output has been predicted using the cell temperature. The inverter efficiency is calculated based on the measured power at the input and output of an inverter. The motor shaft output has been calculated

were  $R$  is a given function,  $w_r$  – the total uncertainty,  $x_1, x_2, \dots, x_n$  – the independent variables,  $w_1, w_2, \dots, w_n$  – the uncertainty in the independent variables. The uncertainties in photovoltaic efficiency, pump efficiency, and overall efficiency are calculated as ±3.2, ±3.8, and ±3.5%, respectively.

#### Modeling of photovoltaic water pumping systems

The detailed modeling procedure of inverter and motor were described earlier research

based on the measured motor input power and the motor speed. The photovoltaic efficiency, pump discharge, pump efficiency, and overall efficiency of the system were calculated based on the predicted cell temperatures for three different modes.

*Performance of a photovoltaic panel*

The cross-section of the photovoltaic laminate is schematically illustrated in fig. 3. It consists of a tempered glass cover with maximum light transmission and minimum heat absorption. The photovoltaic cell is placed at backside of the glass. Two layers of ethyl vinyl acetate were provided above and below the cell for protection. Tedlar is used to improve the strength of the panel and also enhances the life of the panel. Tedlar prevents the moisture infiltration in the cell through the back side of the panel during high humid climates. Heat infiltration from the top surface of the glass and from the bottom surface of tedlar to the cell is due to conduction through the photovoltaic laminate. The properties of panel materials are listed in tab. 4. The energy balance of photovoltaic cell is given by the following equation:

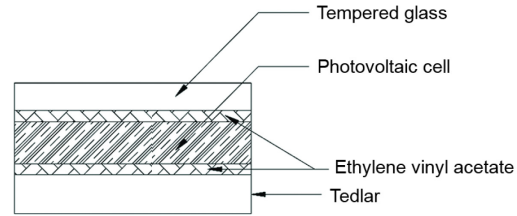


**Figure 3. Cross-section of photovoltaic panel**

**Table 4 Properties of photovoltaic panel materials**

Material	Glass	EVA	Cell	Tedlar
Thickness [mm]	2	0.18	0.5	1
Thermal conductivity [Wm <sup>-2</sup> K <sup>-1</sup> ]	0.98	0.25	148	0.033
Specific heat [kJkg <sup>-1</sup> K <sup>-1</sup> ]	0.8	2.090	0.7	1.09
Density [kgm <sup>-3</sup> ]	2482	960	2328	1720

$$\tau_g \alpha_{cell} G = E + m_{cell} c_{pcell} \left( \frac{dT_{cell}}{dt} \right) + U_{cell-g} (T_{cell} - T_g) + U_{cell-td} (T_{cell} - T_{td}) \quad (2)$$

The heat transfer coefficient between the cell and glass, and cell and tedlar are:

$$U_{cell-g} = \frac{1}{\frac{t_g}{k_g}} \quad (3)$$

$$U_{cell-td} = \frac{1}{\frac{t_{ev}}{k_{ev}} + \frac{t_{td}}{k_{td}}} \quad (4)$$

The energy conversion by the photovoltaic panel is given by:

$$E = \eta_{cell} \tau_g \alpha_{cell} G \quad (5)$$

The efficiency of the cell is given by:

$$\eta_{cell} = \eta_r [1 - \beta(T_{cell} - T_r)] \quad (6)$$

The solution to eq. (2) is given by:

$$T_{cell,i+1} = 0.00275G(t) + 0.77T_{g,i} + 0.229T_{td,i} \quad (7)$$

The net difference between the photocurrent ( $I_{ph}$ ) and the diode current ( $I_d$ ) is [12]:

$$I = \frac{G}{G_{\text{ref}}} [I_{L,\text{ref}} + \mu_{i,\text{sc}}(T_c - T_{c,\text{ref}})] - I_o \left[ \exp\left(\frac{U + IR_s}{AV_t}\right) - 1 \right] \quad (8)$$

The value of  $V_t$  is given by:

$$V_t = \frac{akT_c}{q} \quad (9)$$

The photovoltaic output and electrical efficiency are given by following equations:

$$P_{\text{pv}} = V_{\text{out}} I_{\text{out}} \quad (10)$$

$$\eta_{\text{pv}} = \frac{P_{\text{pv}}}{A_{\text{pv}} G} \quad (11)$$

Fill factor (FF) of a solar cell is the ratio between actual power output of the solar cells to the product of maximum short circuit current and maximum short circuit voltage.

$$FF = \frac{V_m I_m}{V_{\text{oc}} I_{\text{sc}}} \quad (12)$$

The fill factor is in the range between 0.7 and 1.0 [13].

#### *Performance of an inverter*

The inverter converts the direct current photovoltaic output into single phase AC voltage to power the induction motor. The input voltage of the inverter produced by photovoltaic panel fluctuates according to the ambient conditions. However, the inverter delivers the output to the induction motor when the photovoltaic output is more than 30 HZ and more than 200 W [14]. The inverter efficiency is given by:

$$\eta_i = \frac{P_{\text{out}}}{P_{\text{in}}} \quad (13)$$

where  $P_{\text{in}}$  and  $P_{\text{out}}$  are the power input and power output of the inverter.

#### *Brake power of an AC induction motor*

The brake power of an electrical motor is calculated using following relation:

$$\eta_{\text{motor}} = \frac{BP}{E} \quad (14)$$

where motor efficiency is assumed as 0.9.

#### *Performance of a centrifugal pump*

A simplified mathematical model for a centrifugal pump is given by [14]:

$$P(Q) = aQ^3 + bQ^2 + cQ + d \quad (15)$$

where  $P$  is the electrical power consumed by the pump,  $a$ ,  $b$ ,  $c$  and  $d$  are the principal parameters of a pump model. The instantaneous pump discharge can be predicted based on the power

consumed by the pump is obtained from above equation by using Newton-Raphson method or Secant method. After  $i$  iterations, the instantaneous pump discharge is given by:

$$Q_i = Q_{i-1} - \frac{f(Q_{i-1})}{f'(Q_{i-1})} \quad (16)$$

where  $f(Q_{k-1})$  is given by:

$$f(Q_{k-1}) = aQ_{k-1}^3 + bQ_{k-1}^2 + cQ_{k-1} + d - P(Q_{k-1}) \quad (17)$$

The pump efficiency is calculated using following equation:

$$\eta_{\text{pump}} = \frac{c_h Q h}{P_m} \quad (18)$$

#### Prediction of overall system efficiency

The overall system efficiency is defined as the ratio between the hydraulic power output from the pump to the solar energy given to the photovoltaic panel. It is given by:

$$\eta_o = \eta_{\text{pv}} \eta_f \eta_i \eta_m \eta_p \quad (19)$$

The efficiency of cooling fan used for providing cooling effect to the photovoltaic panel is calculated as 0.9.

### Results and discussions

The results obtained from series of experiments with SPVWPS under the influence of panel cooling are discussed in this section. Experimental observations have been made for the period of one month under each mode. However, the experimental observations with similar ambient variations observed on 24<sup>th</sup> day of February 2015 (without the influence of panel cooling), 23<sup>rd</sup> day of March 2015 (cooling above the panel), and 21<sup>st</sup> day of April 2015 (cooling at beneath surface of the panel) were considered for performance comparison. During these days, the similar ambient (such as solar irradiation, ambient temperature and wind velocity) variations were observed.

#### Variation of ambient conditions

The solar irradiation variations during the experimentation with SPVWPS are illustrated in fig. 4. From the figure, it is confirmed that the fluctuations in solar irradiation were observed within 50 W/m<sup>2</sup>. The solar irradiation variations were in the range between 100 and 920 W/m<sup>2</sup>, with an average value of about 520 W/m<sup>2</sup>. The solar irradiation gets increased in the morning hours and gets reduced in the afternoon. A maximum solar irradiation of about 920 W/m<sup>2</sup> was observed on 13.30 hours. The length of sunshine during the experimentation was observed as 11 hours per day. But, the potential sunshine availability is around eight hours per day. The ambient temperature variations are depicted in fig. 5. The ambient temperature has influencing the radiation and convective heat loss from the top surface of the

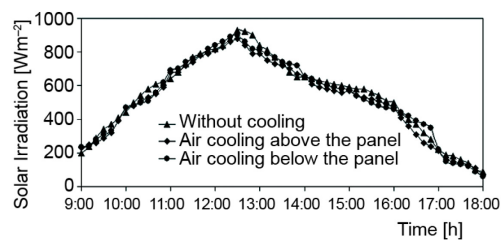


Figure 4. Variation of solar irradiation

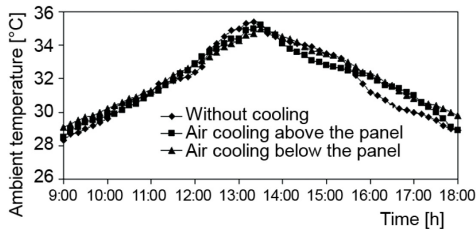


Figure 5. Variation of ambient temperature

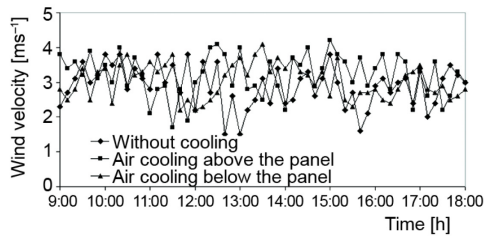


Figure 6. Variation of wind velocity

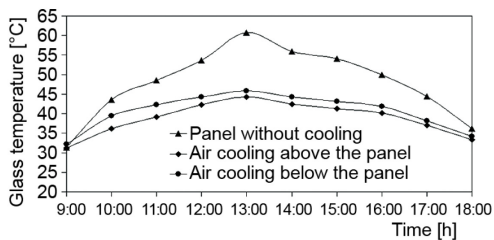


Figure 7. Variation of glass temperature

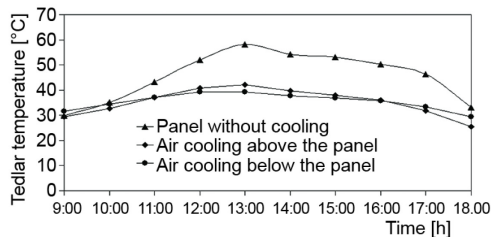


Figure 8. Variation of tedlar temperature

without cooling were in the range between 30.3 and 62.1 °C, with an average temperature of about 48 °C. The cell temperature in the case of panel with cooling at the beneath panel surface was in the range between 30 and 40.1 °C, with an average value of about 35 °C. In the case of cooling above the panel surface, the temperature varied between 30.1 and 43.2 °C, with average value of about 38 °C. The results confirmed that cell temperature was significantly reduced by circulating air over the beneath surface of the panel. The predicted and measured photovoltaic power outputs are compared in fig. 10. The photovoltaic power output (without panel cooling) varied between 200 and 560 W, with an average value of about 350 W. Similarly, the photovoltaic power output in the case of cooling above the panel

photovoltaic panel. During experimentation, the ambient temperature was varied between 28 °C to about 36 °C, with an average value of about 31 °C. Similar ambient temperature variations were observed. The ambient wind velocity variations during experimentation are illustrated in fig. 6. The wind velocity varied in range between 1.5 and 4 m/s, with an average value of 2.4 m/s. The wind velocity is influencing the convective heat loss from the top glass surface of the photovoltaic panel.

#### Performance of a photovoltaic panel

The variations of glass surface temperatures are depicted in fig. 7. The glass surface temperature varied from about 30 to about 62 °C, with an average value of about 47 °C in the case of panel without cooling. Cooling above the glass surface has significantly reduced the average glass temperature from about 47 to about 37 °C. Whereas, cooling of panel over the beneath surface has reduced the average glass temperature from about 47 to about 40 °C. Further, the variations of tedlar temperatures are illustrated in fig. 8. Tedlar temperature was varied from about 30 to about 59 °C, with an average value of about 45 °C in the case of panel without cooling. Panel cooling at the beneath surface has significantly reduced the tedlar temperature variations in the range between 30 and 40 °C, with an average value of about 34 °C. Tedlar temperature variations in the case of panel cooling on the top surface is slightly higher when compared to the panel cooling at the beneath surface. In fig. 9 the variations of predicted cell temperature are illustrated. The cell temperature variations in the case of panel

surface varied between 200 and 590 W, with an average power output of 390 W. The photovoltaic power output in the case of panel cooling over the beneath surface has maximum power output in the range between 200 and 640 W, with an average value of about 410 W. In fig. 11, the variations of photovoltaic efficiency are depicted. The photovoltaic efficiency was varied from 9.5 to 13.5%, from 10.9 to 13.9%, and from 11.8 to 14.4% for the system without cooling, cooling above the panel surface, and cooling over the beneath surface, respectively. The photovoltaic efficiency gets reduced during the peak sunshine hours due to the effect of heating. The panel cooling using air has maintained the cell temperature in the range between 30 and 40 °C, which was found to be about 20 °C lower when compared to the panel without cooling. The efficiency improvements observed in this work are found to be similar to the earlier work [7]. The average fill factor of the photovoltaic panel was calculated as 0.73.

*Performance of an inverter and electrical motor*

The average inverter efficiency was calculated as 0.76 based on the measured power at inverter input and output. The motor brake power was calculated using the motor specifications given by the manufacturer and the speed measured experimentally. The motor brake power for different photovoltaic output was calculated using the average steady state motor efficiency of 0.8.

*Performance of a centrifugal pump*

The pump discharge variations are compared in fig. 12. From the figure, it is confirmed that pump discharge was improved by cooling the panel surfaces. The cooling arrangement provided at the beneath of the panel has enhanced the pump discharge to about 1.35 m<sup>3</sup>/h, which is found to be about 0.4 m<sup>3</sup>/h higher when compared to the SPVWPS without cooling. The variation of pump subsystem efficiency is illustrated in fig. 13. The pump subsystem efficiency was varied from 10 to 22% for the case of system without cooling arrangement, 10.5 to 23.5% for the case of panel with cooling arrangement above the panel. In the case of panel with cooling arrangement provided at the beneath of the panel has attained a maximum efficiency of 24.8%.

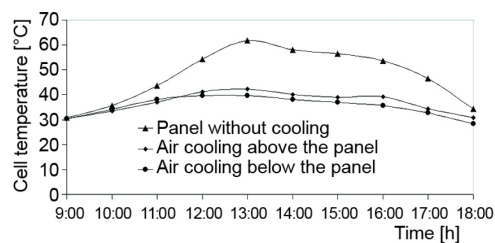


Figure 9. Variation of cell temperature

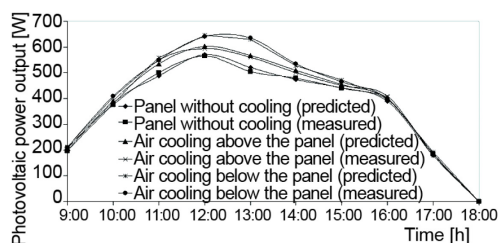


Figure 10. Variation of photovoltaic power output

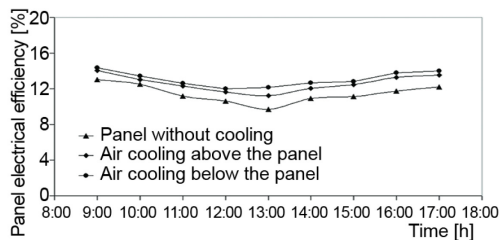


Figure 11. Variation of photovoltaic efficiency

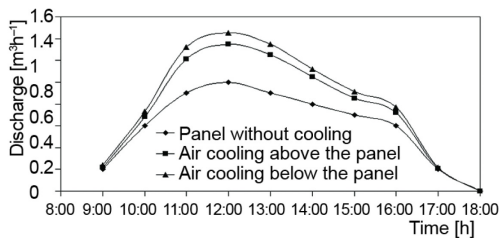


Figure 12. Variation of pump discharge

### Performance of an overall system

The overall efficiency of the SPVWPS system is depicted in fig. 14. The overall efficiency was varied between 1.2 and 1.8%, 1.4 and 2.8%, and 1.6 and 3.5%, for the system without panel cooling, with panel cooling on top surface and with panel cooling at the beneath surface, respectively. The overall system efficiency under the influence of panel cooling over the beneath surface was found to be about 1.8% higher when compared to the system without cooling, which is found to be higher when compared to the earlier work [4].

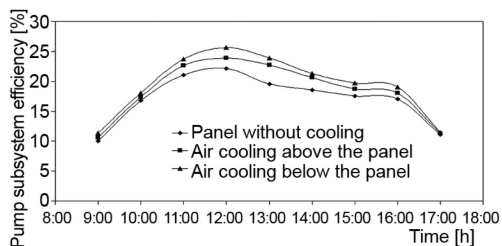


Figure 13. Variation of pump subsystem efficiency

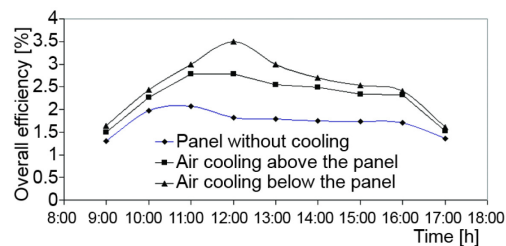


Figure 14. Variation of overall system efficiency

### Parameteric analysis

The influence of photovoltaic cell temperature on the performance of SPVWPS is illustrated in fig. 15. An increase in photovoltaic cell temperature has significantly reduced the photovoltaic electrical conversion efficiency, pump sub system efficiency and overall system efficiency by about 6, 10, and 1.4%, respectively at constant solar irradiation of  $600 \text{ W/m}^2$  with a pumping head of 15 m. Similarly, the influence of solar irradiation on the performance of a SPVWPS at constant cell temperature of  $35 \text{ }^\circ\text{C}$  and 15 m pumping head is illustrated in fig. 16. An increase in solar irradiation has significantly improved the efficiency of the photovoltaic panel, pump subsystem, and overall system by about 4.5, 11, and 1.2%, respectively.

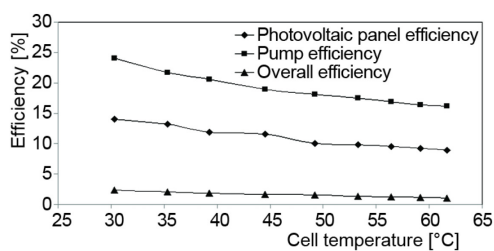


Figure 15. Influence of cell temperature at  $600 \text{ W/m}^2$  and 15 m head

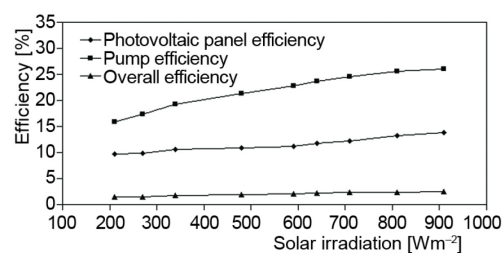


Figure 16. Influence of solar irradiation at cell temperature  $35 \text{ }^\circ\text{C}$  and 15 m head

### Conclusions

The performance of a SPVWPS was evaluated under the influence of panel cooling. Based on the investigations, following major conclusions are arrived.

- The photovoltaic cell temperature was significantly reduced from about  $62 \text{ }^\circ\text{C}$  to about  $35 \text{ }^\circ\text{C}$ , and  $38 \text{ }^\circ\text{C}$  in the case of air cooling arrangement provided at the beneath surface of the panel and air cooling arrangement above the panel surface, respectively.

- The theoretically predicted photovoltaic power output (based on the measured glass and tedlar temperatures) was found to be closer to the experimental results with  $\pm 5\%$  deviations.
- The photovoltaic efficiency, pump subsystem efficiency and system efficiency are enhanced by about 3.5, 2.5, and 1.8%, respectively.
- The results confirmed that cooling arrangement provided at the beneath surface of the panel has better performance improvement when compared to the cooling arrangement above the panel.

### Nomenclature

$A$	– quality factor
$A_{pv}$	– photovoltaic area, [m <sup>2</sup> ]
$a$	– diode ideality factor
BP	– shaft power output, [W]
$c_p$	– specific heat, [kJkg <sup>-1</sup> K <sup>-1</sup> ]
$E$	– photovoltaic output, [W]
$G$	– global solar radiation, [Wm <sup>-2</sup> ]
$G_{ref}$	– reference condition (= 1000 W/m <sup>2</sup> )
$I_{L,ref}$	– light current at reference condition, [A]
$I_m$	– measured current, [A]
$I_o$	– reverse saturation current, [A]
$I_{out}$	– output current of the cell, [A]
$I_{sc}$	– short circuit current, [A]
$K$	– Boltzmann constant
$m_{cell}$	– mass of the cell material, [kg]
$P_{pv}$	– photovoltaic power output, [W]
$Q$	– pump discharge, [m <sup>3</sup> h <sup>-1</sup> ]
$q$	– electron charge
$R_s$	– series resistance
$T_c$	– cell temperature, [K]
$T_g$	– glass temperature, [K]
$T_r$	– reference temperature (= 298 K)
$T_{td}$	– tedlar temperature, [K]
$U_{cell-td}$	– heat transfer coefficient, [Wm <sup>-2</sup> K <sup>-1</sup> ]
$V_m$	– maximum open circuit voltage, [V]
$V_{oc}$	– open circuit voltage, [V]
$V_{out}$	– output voltage of the cell, [V]

### Greek symbols

$\beta$	– temperature coefficient
$\eta_i$	– efficiency of an inverter
$\eta_m$	– efficiency of a motor
$\eta_o$	– overall efficiency of the pump
$\eta_p$	– efficiency of a pump
$\eta_{pv}$	– efficiency of the photovoltaic panel
$\eta_r$	– reference efficiency (= 0.18)
$\mu_{i,sc}$	– temperature coefficient short circuit current, [A°C <sup>-1</sup> ]
$\tau_g$	– transmissivity of the glass

### Subscripts

c	– cell
ev	– ethyl vinyl acetate
f	– fan
g	– glass
h	– hydraulic
i	– inverter
m	– measured
oc	– open circuit
p	– pump
pv	– photovoltaic
ref	– reference
r	– relative
sc	– short circuit
td	– tedlar

### References

- [1] Gopal, C., et al., Renewable Energy Based Water Pumping Systems – A Literature Review, *Renewable and Sustainable Energy Reviews*, 25 (2013), Sept., pp. 351-370
- [2] Sontake, V. C., Kalamkar, V. R., Solar Photovoltaic Water Pumping System – A Comprehensive Review, *Renewable and Sustainable Energy Reviews*, 59 (2016), June, pp. 1036-1067
- [3] Tabaei, H., Ameri, M., The Effect of Booster Reflectors on the Photovoltaic Water Pumping System Performance, *Journal of Solar Energy Engineering*, 134 (2012), 1, pp. 1-4
- [4] Abdolzadeh, M., Ameri, M., Improving the Effectiveness of a Photovoltaic Water Pumping System by Spraying Water over the Front of Photovoltaic Panels, *Renewable Energy*, 34 (2009), 1, pp. 91-96
- [5] Habibollahi, M., et al., Efficiency Improvement of Photovoltaic Water Pumping System by Means of Water Flow beneath Photovoltaic Cells Surface, *Journal of Solar Energy Engineering*, 137 (2015), 4, pp. 1-8
- [6] Kordzadeh, A., The Effects of Nominal Power of Array and System Head on the Operation of Photovoltaic Water Pumping Set with Array Surface Covered by a Film of Water, *Renewable Energy*, 35 (2010), 5, pp. 1098-1102

- [7] Teo, H. G., et al., An Active Cooling System for Photovoltaic Modules, *Applied Energy*, 90 (2012), 1, pp. 309-315
- [8] Nizetic, S., et al., Water Spray Technique Applied on a Photovoltaic Panel: The Performance. *Energy Conversion and Management*, 108 (2016), Jan., pp. 287-296
- [9] Holman, J. P., *Experimental Methods for Engineers*, Tata McGraw Hill Publishing Company, New Delhi, 2007
- [10] Chenni, R., et al., A Detailed Modeling Method for Photovoltaic Cells, *Energy*, 32 (2007), 9, pp. 1724-1730
- [11] Chancrasekaran, N., Thyagarajah, K., Simulation and Experimental Validation of AC Motor and PMDC Motor Pumping System Fed by Photovoltaic Cell, *Indian Journal of Engineering and Materials Sciences*, 21 (2014), Feb., pp. 93-103
- [12] Jafar, M., A Model for Small Scale Photovoltaic Solar Water Pumping System, *Renewable Energy*, 19 (2000), 1-2, pp. 85-90
- [13] Hamidat, A., Benyoucef, B., Mathematic Models of Photovoltaic Motor-Pump Systems, *Renewable Energy*, 33 (2008), 5, pp. 933-942
- [14] Daud, A-K., Mahmoud, M. M., Solar Powered Induction Motor-Driven Water Pump Operating on a Desert Well, Simulation and Field Tests, *Renewable Energy*, 30 (2005), 5, pp. 701-714